

Optical properties of microcrystalline materials

M. Vaněček^{a,*}, A. Poruba^a, Z. Remes^a, N. Beck^b, M. Nesladek^c

^a Institute of Physics, Academy of Sciences of the Czech Republic, Cukrovarnická 10, CZ-16200 Praha 6, Czech Republic

^b Institute of Microtechnology, Neuchatel University, Rue A.-L. Breguet 2, CH-2000 Neuchatel, Switzerland

^c Institute for Materials Research, Limburgs University, B-3590 Diepenbeek, Belgium

Abstract

We use optical, photocurrent and photothermal deflection spectroscopies to study defects in microcrystalline silicon ($\mu\text{c-Si}$) thin films and diamond layers. Enhanced light absorption in $\mu\text{c-Si}$ films and solar cells is due to several contributions: light scattering, change in the optical transition probability for strained and surface atoms and residual amorphous fraction. Low defect density (optical absorption with a coefficient, α , smaller than 0.1 cm^{-1} at about 0.8 eV , as measured by the constant photocurrent method), amorphous volume fraction below 10% and a distinct surface texture is typical for a material yielding a good efficiency $\mu\text{c-Si}$ solar cells. Main defects in heteroepitaxial chemical vapor deposition diamond films are discussed.

Keywords: Microcrystalline silicon; Thin films; Diamonds

1. Introduction

Materials with micrometer and nanometer crystallites constitute an important class, with some of their properties distinctly different from either amorphous or large grain material and single crystals. Especially, thin silicon films of nanometer and micrometer crystallites are interesting for their optoelectronic and photovoltaic applications.

Microcrystalline silicon ($\mu\text{c-Si}$) p-i-n solar cells have recently been introduced as the bottom cell of an amorphous silicon (a-Si)/ $\mu\text{c-Si}$ tandem cell [1]. Intrinsic microcrystalline layers, deposited by very high frequency glow discharge (VHF-GD), have a

small subgap (defect-connected) absorption and three to four times increase in optical absorption as compared to crystalline silicon. Light scattering, shift of the indirect optical gap due to internal mechanical strain, absorption from surface states as well as amorphous volume fraction have all been suggested as a possible source for this increase [2].

Results of optical investigation of $\mu\text{c-Si}$ and CVD diamond films will be presented here. Since layers frequently have rough or textured surfaces, its affect on light scattering has been investigated.

2. Experimental

Microcrystalline silicon layers and solar cells were deposited at IMT, Neuchatel University by VHF-GD, using silane diluted in hydrogen, with and without a

* Corresponding author. Tel.: +420-2 24311137; fax: +420-2 8123184; e-mail: vanecek@fzu.cz

gas purifier [1,3,4]. Layers were deposited on a glass substrate with typical thickness between 2 and 3 μm .

Diamond films were grown at IMO, Limburgs University by plasma-enhanced chemical vapor deposition (PECVD) in a microwave plasma reactor (Astex PDS-17) from a methane/hydrogen/oxygen mixture [5]. Silicon wafers were used as a substrate material. After deposition, the Si substrate was etched away and self-supporting films, 10 to 450 μm thick, were used for the optical measurements.

A computer-controlled single-beam spectrometer was used for transmittance/reflectance measurements in the 0.6–5.5 eV spectral region, with and without an integrating sphere. Absorbance was measured directly with the help of photothermal deflection spectroscopy (PDS) [6], and with the constant photocurrent method (CPM) [7]. CPM was used both in the standard mode and in the ‘Absolute CPM’ mode [8]. Coplanar Al or Cr electrodes were evaporated onto the layers with the interelectrode spacing varying from 30 μm to 3 mm.

3. Results

3.1. Evaluation of light scattering

The spectral dependence of the transmittance of a typical $\mu\text{c-Si}$ layer is shown in Fig. 1. An integrating sphere with a detector is placed either close to or

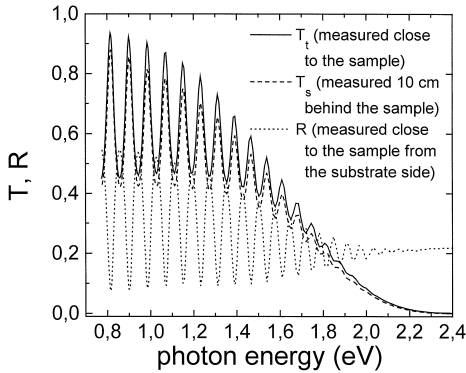


Fig. 1. Transmittance T and reflectance R spectra of a typical textured microcrystalline Si layer, deposited by VHF-GD.

far behind the sample. We can see well-defined interference fringes. Modulation depth in a non-absorbing region is given by the index of refraction and for a ‘slightly milky, not mirror-like’ sample it is reduced due to some light scattering. Evaluation of the extinction coefficient, $\alpha_{\text{ext}}(E)$, given as sum, $\alpha(E) + \alpha_{\text{sc}}(E)$, to $E = 1$ eV, where the (true) optical absorption coefficient, $\alpha(E)$, of silicon is much smaller, gives us a good estimate for the scattering coefficient, $\alpha_{\text{sc}}(E)$. Surface roughness has been measured with a surface profilometer and by comparison of the measured specular reflectance of the free (rough) surface and the (smooth) silicon/glass interface. From the latter measurement, the root mean square value of surface roughness and the spectral dependence of $\alpha_{\text{sc}}(E)$ can be directly calculated [9]. Approximate knowledge of $\alpha_{\text{sc}}(E = 1 \text{ eV})$ and its spectral dependence (between E^4 and E^2 [10,11]) is then used for the evaluation of the optical absorption coefficient, $\alpha(E)$.

Evaluation of the scattering coefficient from transmittance/reflectance measurement is possible for our 2- μm thin films, if the optical scattering coefficient $\alpha_{\text{sc}} \geq 100 \text{ cm}^{-1}$. We have measured α_{sc} (at $E = 1$ eV) between 200 and 400 cm^{-1} for our textured VHF-GD layers, deposited under similar conditions as our $\mu\text{c-Si}$ solar cells with 5 to 7% efficiency, α_{sc} increases with photon energy as $E^2 - E^3$. These layers have a texture similar to SnO_2 on glass (Asahi, type U). On the other hand, for the mirror-like microcrystalline layers, with no suppression of interference fringes, α_{sc} is smaller than about 50 cm^{-1} in the IR region.

For evaluation of the ‘true’ $\alpha(E)$ and the defect-connected, (typically very small) subgap optical absorption in thin films of $\mu\text{c-Si}$ deposited by VHF-GD, we need a method which measures directly absorbance in the film down to 10^{-6} . Both PDS and CPM, well known from the field of amorphous silicon, can be used [6,7]. They give us an ‘apparent’ optical absorption coefficient $\alpha_{\text{app}}(E)$, affected by scattering. The sensitivity of PDS is limited due to non-negligible substrate absorption. Hence, we have preferred CPM for evaluation of the scattering coefficient and a low defect absorption (absorbance below 10^{-4}). In CPM we detect the light absorbed (either directly or after one or more scattering events) in between the electrodes used for a photocurrent

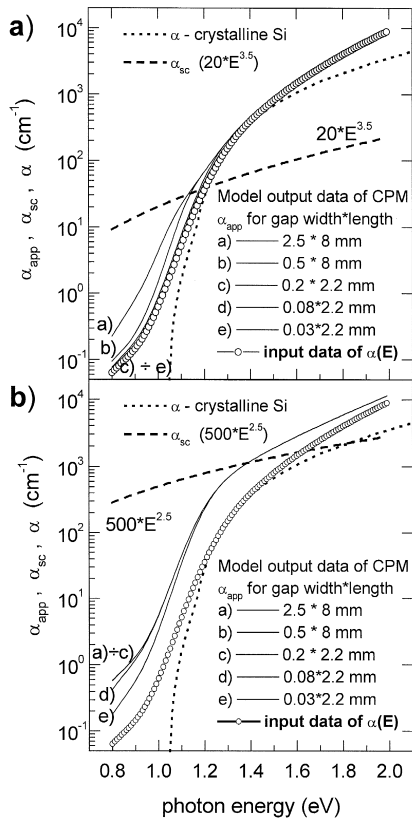


Fig. 2. 'Apparent' CPM optical absorption coefficient, calculated from the model input data of 'true' $\alpha(E)$, for the different scattering coefficients (a) $\alpha_{sc} = 20 E^{3.5}$ and (b) $\alpha_{sc} = 500 E^{2.5}$, as a function of the interelectrode spacing; $\alpha(E)$ of the crystalline silicon is shown, too.

measurement. By changing the spacing between the electrodes by two orders of magnitude, we can vary the contribution of light scattering upon the measured, 'apparent' optical absorption coefficient α_{app} . For the case of a mirror-like amorphous silicon [12], with a typical α_{sc} between 0.1 and 10 cm⁻¹ we have presented a theory for evaluation of α_{sc} and $\alpha(E)$ in Refs. [12,13]. For the case of our μc -Si, which is less homogeneous and frequently textured, the values of α_{sc} are much larger and a more general theory is needed.

Our theory is based on multiple scattering (in the bulk and at a rough surface) in the layer of μc -Si: only the light within the escape cone (given by refractive index of Si and surrounding medium), or absorbed (after scattering) outside the region of elec-

tric field between the electrodes for CPM photocurrent measurement, gives no contribution to the constant photocurrent [14]. For smaller scattering (mirror-like surface and a negligible void fraction) the 'apparent' absorption coefficient measured by CPM with electrodes whose length and width are the smallest approaches quite close to the 'true' optical absorption coefficient, as seen from model data in Fig. 2a). For strong surface scattering ('milky' appearance), the apparent absorption coefficient saturates for all gaps greater than 0.2 mm, as can be seen from Fig. 2b). Here, the 'true' optical absorption coefficient is about 10 times less than the 'apparent' one at 0.8 eV (in the region of the smallest defect absorption). This enhancement reaches its largest possible value, given by the indices of refraction of the microcrystalline Si layer, n_{Si} , and glass substrate, n_{glass} , and equal to $2(n_{Si}/n_{glass})^2 \cong 10$. For a rough silicon layer with air on both sides it reaches the value of $2n_{Si}^2$ [15].

3.2. Optical absorption in microcrystalline silicon

CPM was used to measure the optical absorption coefficient of mirror-like and 'milky' thin layers. Fig. 3 shows how the 'true' α is obtained from experimental CPM and transmittance data. The mea-

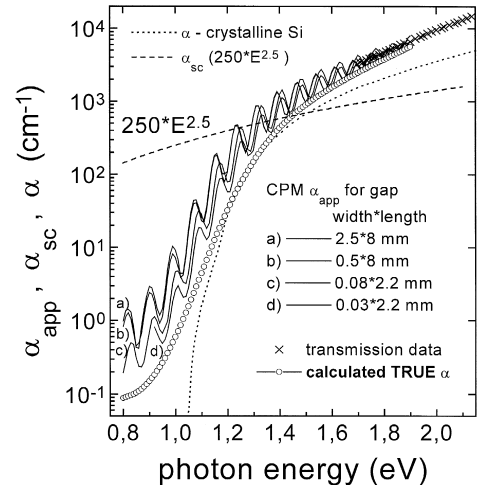


Fig. 3. CPM spectra α_{app} of a textured microcrystalline layer measured with different interelectrode spacing, and 'true' $\alpha(E)$ (circles) calculated from our model; $\alpha(E)$ of crystalline silicon is shown for comparison (dotted line).

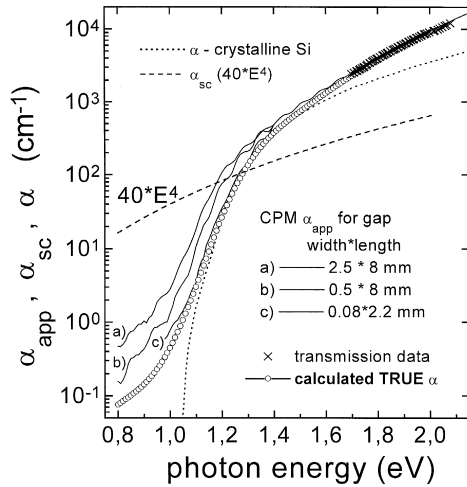


Fig. 4. Absolute CPM spectra α_{app} of a mirror-like μc -Si film and ‘true’ $\alpha(E)$ evaluated from all CPM data. Here the $\alpha_{app}(E)$ approaches the $\alpha(E)$ for 80 μm spacing between the evaporated electrodes.

sured sample had a ‘milky’ appearance due to surface texture. CPM was measured at different widths between the coplanar electrodes; narrow electrodes have also a shorter length. These measurements gives us the ‘apparent’ optical absorption coefficients, $\alpha_{app}(E)$. Transmittance/reflectance data have been used to estimate $\alpha_{sc}(E)$, as discussed at the beginning of previous paragraph.

Results for a mirror-like layer are shown in Fig. 4. Here, the ‘absolute’ CPM measurement with the smallest interelectrode spacing can give directly the $\alpha(E)$ spectrum.

3.3. Optical and photocurrent spectroscopy of diamond self-supporting layers

Defect-induced optical absorption in undoped CVD diamond layers is shown in Fig. 5. PDS has been used to measure $\alpha(E)$ [5]. Spectra were set to the absolute scale by transmittance/reflectance measurement, the highest quality sample (4i) is thick (450 μm) and polished.

Photocurrent spectra (ac measurement at 10 Hz) of samples with a different nitrogen content are shown also in Fig. 5. The spectra have been normalized for the light intensity and matched with PDS data at 5.5 eV. Details are presented elsewhere [16].

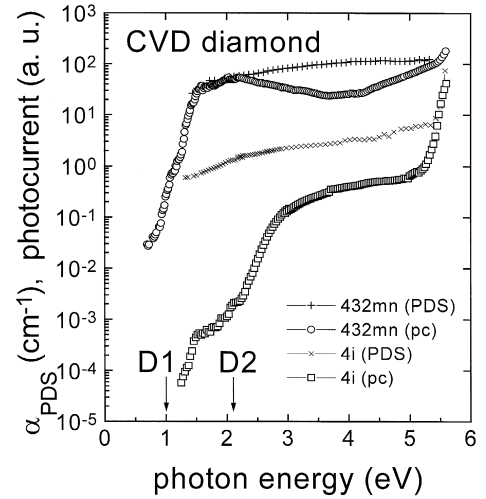


Fig. 5. Optical absorption coefficient α , as measured by PDS for the best undoped (4i) and N doped (432 mn) samples. Photocurrent spectra (pc), normalized for the light intensity and matched at 5.5 eV to PDS data are shown, too.

The sample (4i) has only residual nitrogen contamination, sample (432 mn) is nitrogen doped.

Two threshold energies for the optical transitions are seen in sample (4i): D1 at about 1 eV and D2 at approximately 2.1 eV. Only the transition D1 is observed in the nitrogen doped sample similar to the observation in Ref. [17].

4. Discussion

4.1. Microcrystalline silicon

The spectral dependence of the optical absorption coefficient, $\alpha(E)$, is due to the specific properties of μc -Si (band structure, defect states). Figs. 3 and 4 show that between 1.2 and 1.4 eV, $\alpha(E)$ (true) of microcrystalline and crystalline Si is nearly the same (for μc -Si deposited by VHF-GD, mirror-like or textured, for the latter with a larger experimental error possible). This region determines the magnitude of the indirect gap.

We observe an exponential tail around 1.1 eV, with a slope slightly less than 50 meV. This energy we interpret as a disorder-induced broadening of the indirect absorption edge of c-Si [18].

In Fig. 6 we plot the optical absorption coefficient of crystalline and amorphous silicon, together with the optical absorption coefficient for the amorphous/crystalline mixture. We calculated the amorphous/crystalline mixture with the help of the effective medium approximation [19], and knowing the amorphous fraction of our sample (below 10% for the sample presented in Fig. 3, as determined by Raman scattering [14]). We note that only a part of the increase in α above 1.4 eV, compared to the c-Si, can be explained by the contribution from the amorphous fraction and other mechanisms must be evoked. Because of a high internal strain in our samples (as detected by Raman spectroscopy and substrate curvature method) and because of a large number of surface Si atoms (needle-like oriented grains with a diameter about 15 nm) [1,3] we explain this enhancement by an increase in the optical transition probability for those Si atoms in the investigated spectral region.

In the subgap spectral region, defect-connected absorption is observed. This absorption generally increases with a hydrogen evolution (we have about 5% H in ‘as grown’ material) and decreases with hydrogenation. Silicon dangling bonds, as identified by electron spin resonance, have been suggested as

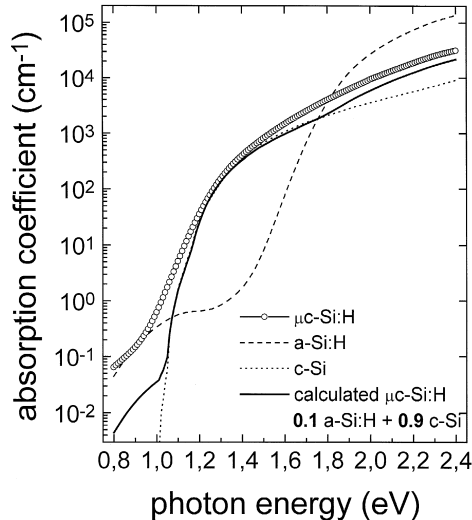


Fig. 6. Comparison of the optical absorption coefficients of c-Si, μ c-Si, a-Si and calculated α with the help of effective media approximation (10% a-Si and 90% c-Si).

the dominant defects responsible for this absorption [2,20].

We also investigated the effect of oxygen, in the range 10^{18} to 10^{20} atoms/cm³ [4]. We observed changes in the film texture and amorphous fraction with use of oxygen purifier, but no changes in the defect-connected absorption, as seen from comparison of Figs. 3 and 4. Here, only the oxygen concentration differs by two orders of magnitude. Hence, oxygen either contributes to the passivation of grain boundaries, as known from monocrystalline Si, or the number of oxygen-connected deep defects does not surpass the number of surface dangling bonds.

From the point of view of the solar cell efficiency, two important parameters are mentioned below.

(1) The value of the ‘true’ $\alpha(E)$ in the subgap absorption (defect-connected) region. Good solar cells investigated so far have $\alpha(E = 0.8 \text{ eV})$ below 0.1 cm^{-1} . If the optical cross section of the silicon dangling bond is similar to its value in amorphous hydrogenated silicon, then this absorption corresponds to $\approx 10^{15}$ dangling bonds/cm³ in our ‘mid-gap’ samples (with the Fermi level in the middle of the gap) [20,21].

(2) The ‘apparent’ optical absorption coefficient, α_{app} , in the spectral range above 1.1 eV, as measured by CPM with widely spaced coplanar electrodes determines the absorptance within a solar cell, the effect of light scattering is fully included. Calculated and measured spectral response are in a good agreement [14].

4.2. Characteristic defects in CVD diamond films

Clusters of sp^2 bonded carbon are the main defect in a sp^3 diamond structure [5,17]. Raman scattering is routinely used as a characterization method. With improvement in CVD diamond growth, Raman scattering (excited by blue or green laser lines) does not detect sp^2 bonded carbon and we have demonstrated that PDS can be more sensitive in detecting residual sp^2 carbon and/or carbon dangling bonds [5].

Residual nitrogen is always present in CVD diamond films [17]. If nitrogen is in a single substitutional form, as in the Ib diamond [17], we can observe its characteristic optical transition to the conduction band in the photocurrent spectrum, with

threshold energy ≈ 2.1 eV [16]. This D2 level was recently confirmed by photoemission spectroscopy [22]. Nitrogen doping (and decrease in Raman quality factor) lead to a shift of the threshold energy to about 1 eV [16]. ESR measurements are in progress to clarify the origin of this D1 level (carbon dangling bond, ≈ 1 eV above the valence band?).

5. Conclusions

Enhanced light absorption in $\mu\text{c-Si}$ textured layers is due to a light scattering; an additional enhancement for all layers comes from a change in the optical transition probability for strained and surface atoms and from a residual amorphous fraction. Low defect density (characterized by α smaller than 0.1 cm^{-1} at about 0.8 eV, as measured by CPM), amorphous volume fraction below 10% and a distinct surface texture is typical for a material yielding good efficiency $\mu\text{c-Si}$ solar cells. The main characteristic defects in heteroepitaxial CVD diamond films are clusters of sp^2 bonded carbon, residual nitrogen and presumably carbon dangling bonds.

Acknowledgements

This work was supported by E.C. contract JOR3-CT97-0145 and by the grant 202/96/0446 of the Grant agency of the Czech Republic.

References

[1] J. Meier, S. Dubail, D. Fischer, J.A. Anna Selvan, N. Pellaton Vaucher, R. Platz, Ch. Hof, R. Fluckiger, U. Kroll, N.

- Wyrsh, P. Torres, H. Keppner, A. Shah, K.D. Ufert, Proc. 13th European PV Conf., Nice, 1995, p. 1445.
- [2] N. Beck, J. Meier, J. Fric, Z. Remeš, A. Poruba, R. Fluckiger, J. Pohl, A. Shah, M. Vaněček, J. Non-Cryst. Solids 198–200 (1996) 903.
- [3] J. Meier, R. Fluckiger, H. Kepner, A. Shah, Appl. Phys. Lett. 65 (1994) 860.
- [4] P. Torres, J. Meier, R. Fluckiger, U. Kroll, J.A. Anna Selvan, H. Kepner, A. Shah, S.D. Littlewood, I.E. Kelly, P. Giannoulas, Appl. Phys. Lett. 69 (1996) 1373.
- [5] M. Nesládek, K. Meykens, L.M. Stals, M. Vaněček, J. Rosa, Phys. Rev. B 54 (1996) 5552.
- [6] W.B. Jackson, N.M. Amer, A.C. Boccara, D. Fournier, Appl. Opt. 20 (1983) 1333.
- [7] M. Vaněček, J. Kocka, J. Stuchlík, Z. Kozisek, O. Stika, A. Triska, Solar Energy Mater. 8(1983) 411.
- [8] M. Vaněček, J. Koecká, A. Poruba, A. Fejfar, J. Appl. Phys. 78 (1995) 6203.
- [9] Z. Yin, H.S. Tan, F.W. Smith, Diamond Related Mater. 5 (1996) 1490.
- [10] M. Bass (Ed.), Handbook of Optics, Vol. 1, 2nd edn., McGraw-Hill, New York, 1995.
- [11] H.C. Van de Hulst, Light Scattering by Small Particles, Wiley, New York, 1957.
- [12] M. Favre, H. Curtins, M. Vaněček, J. Non-Cryst. Solids 114 (1989) 405.
- [13] M. Vaněček, J. Holoubek, A. Shah, Appl. Phys. Lett. 59 (1991) 2237.
- [14] A. Poruba, A. Fejfar, J. Kocka, V. Vorlíček, M. Vaněček, N. Beck, P. Torres, J. Meier, A. Shah, to be published.
- [15] E. Yablonovitch, G.D. Cody, IEEE Trans. Electron Devices ED 29 (1982) 300.
- [16] M. Nesládek, L.M. Stals, J.M. Marshall, S. Roberson, presented at Diamond 1997, Edinburgh.
- [17] E. Rohrer, C.F.O. Graeff, R. Janssen, C.E. Nebel, M. Stutzmann, H. Guttler, R. Zachai, Phys. Rev. B 54 (1996) 7874.
- [18] G.D. Cody, J. Non-Cryst. Solids 141 (1992) 3.
- [19] L. Ward, The Optical Constants of Bulk Materials and Films, 2nd edn., IOP Publ., Bristol, 1994, p. 246.
- [20] W.B. Jackson, N.M. Johnson, D.K. Biegelsen, Appl. Phys. Lett. 43 (1983) 195.
- [21] N. Wyrsh, F. Finger, T.J. McMahon, M. Vaněček, J. Non-Cryst. Solids 137–138 (1991) 347.
- [22] J. Ristein, W. Stein, L. Ley, Phys. Rev. Lett. 78 (1997) 1803.